Monthly Notices of the ROYAL ASTRONOMICAL SOCIETY

MNRAS **506,** 4654–4666 (2021) https://doi.org/10.1093/mnras/stab2032
Advance Access publication 2021 July 21

Ultracompact X-ray binaries with He star companions

Bo Wang [1]★ Wen-Cong Chen [2,3]★ Dong-Dong Liu,[1] Hai-Liang Chen,[1] Cheng-Yuan Wu,[4] Wen-Shi Tang,[5] Yun-Lang Guo[1] and Zhan-Wen Han [1]★

[1]*Yunnan Observatories, Chinese Academy of Sciences, Kunming 650216, China*
[2]*School of Science, Qingdao University of Technology, Qingdao 266525, China*
[3]*School of Physics and Electrical Information, Shangqiu Normal University, Shangqiu 476000, China*
[4]*Physics Department and Tsinghua Center for Astrophysics, Tsinghua University, Beijing 100084, China*
[5]*School of Astronomy and Space Science, Nanjing University, Nanjing 210023, China*

Accepted 2021 July 12. Received 2021 July 12; in original form 2021 February 23

ABSTRACT

Ultracompact X-ray binaries (UCXBs) are low-mass X-ray binaries with hydrogen-deficient mass donors and ultrashort orbital periods. They have been suggested to be the potential *Laser Interferometer Space Antenna* (*LISA*) sources in the low-frequency region. Several channels for the formation of UCXBs have been proposed so far. In this paper, we carried out a systematic study on the He star donor channel, in which a neutron star (NS) accretes matter from a He main-sequence (MS) star through Roche lobe overflow, where the mass transfer is driven by the gravitational wave radiation. First, we followed the long-term evolution of the NS+He MS binaries by employing the stellar evolution code Modules for Experiments in Stellar Astrophysics (MESA), and thereby obtained the initial parameter spaces for the production of UCXBs. We then used these results to perform a detailed binary population synthesis approach to obtain the Galactic rates of UCXBs through this channel. We estimate the Galactic rates of UCXBs appearing as *LISA* sources to be $\sim$3.1–11.9 Myr^{-1} through this channel, and the number of such UCXB-*LISA* sources in the Galaxy can reach about 1–26 calibrated by observations. This work indicates that the He star donor channel may contribute significantly to the Galactic UCXB formation rate. We found that the evolutionary tracks of UCXBs through this channel can account for the location of the five transient sources with relatively long orbital periods quite well. We also found that such UCXBs can be identified by their locations in the mass-transfer rate versus the orbital period diagram.

Key words: gravitational waves – binaries: close – stars: evolution – X-rays: binaries.

1 INTRODUCTION

Ultracompact X-ray binaries (UCXBs) are a subtype of low-mass X-ray binaries (LMXBs), containing a compact accretor and a hydrogen-deficient mass donor with an ultrashort orbital period (usually less than 1 h; for a review see Nelemans & Jonker 2010). They are a kind of accretion-powered X-ray sources, in which the accretor could be a neutron star (NS) or a stellar-mass black hole (BH) that is accreting matter from a mass donor through Roche lobe overflow (RLOF; e.g. Savonije, de Kool & van den Heuvel 1986). So far, there are about 40 known UCXBs or candidates, in which 15 of them have been identified with high confidence on the basis of the observed orbital periods (including 10 persistent sources and five transient sources; see e.g. in't Zand, Jonker & Markwardt 2007; Liu, van Paradijs & van den Heuvel 2007; Cartwright et al. 2013; Heinke et al. 2013; Pietrukowicz et al. 2019; Coti Zelati et al. 2021; Peng & Shen 2021). It has been suggested that all confirmed UCXBs contain NS accretors, but the nature of accretors has not been identified exclusively in the observations (e.g. Sazonov et al. 2020; Coti Zelati et al. 2021).[1] To date, about a third of observed UCXBs have been found in dense globular clusters that can enhance UCXB production owing to dynamical interactions, such as tidal captures or stellar encounters (see e.g. Bailyn & Grindlay 1987; Verbunt 1987; Davies, Benz & Hills 1992; Davies & Hansen 1998; Ivanova et al. 2005, 2010).

UCXBs play an important role in broad aspects of astrophysics, as follows. (1) UCXBs have been thought to be strong continuous gravitational wave (GW) sources in the low-frequency region ($\sim 10^{-4}$–10^{-3} Hz), which can be detected by the space GW detectors, such as *Laser Interferometer Space Antenna* (*LISA*; e.g. Nelemans 2009; Amaro-Seoane et al. 2017; Tauris 2018), *Taiji* (e.g. Luo et al. 2020; Ruan et al. 2020, 2021), and *TianQin* (e.g. Luo et al. 2016; Bao et al. 2019; Wang et al. 2019; Huang et al. 2020), etc. (2) UCXBs provide important constraints on the binary evolution, such as the angular momentum loss mechanisms, the common-envelope evolution, and the mass-accretion process of compact objects, etc. (e.g. Zhu, Lü & Wang 2012). (3) UCXBs are excellent astrophysical laboratories, since they are interesting X-ray sources and also the

★ E-mail: wangbo@ynao.ac.cn (BW); chenwc@pku.edu.cn (WCC); zhanwenhan@ynao.ac.cn (ZWH)

[1]UCXBs with BH accretors have not been confirmed, but there is a known moderately strong BH UCXB candidate 47 Tuc X9 in our Galaxy (see Bahramian et al. 2017; Tudor et al. 2018).

combination of ultrashort orbital periods, compact accretors, and mass donors with different chemical compositions (e.g. Nelemans & Jonker 2010; Lin & Yu 2018). (4) UCXBs have been proposed to be progenitor candidates of millisecond radio pulsars (see Alpar et al. 1982).

Because of the ultrashort orbital periods, the mass donors in UCXBs could be constrained to be hydrogen deficient, partially or fully degenerate stars, such as white dwarfs (WDs) or non-degenerate naked He stars (e.g. Rappaport, Joss & Webbink 1982; Nelson, Rappaport & Joss 1986; Bisnovatyi-Kogan 1989; Deloye & Bildsten 2003; Zhong & Wang 2011).[2] The spectra in some UCXBs indicate that the accreted matter on to NSs mainly consists of helium or carbon and oxygen, which may help to identify the mass donors (e.g. Nelemans et al. 2004; Nelemans, Jonker & Steeghs 2006). Especially, thermonuclear (Type I) X-ray bursts on the surface of NSs show distinct features in dependence of the accreted matter, which can be used to constrain the compositions of the mass donors in UCXBs (see e.g. Cumming 2003; Galloway et al. 2008). van Haaften, Voss & Nelemans (2012c) recently obtained the compositions of the mass donors in 10 UCXBs, in which about half of them are likely to be rich in helium.

Up to now, several channels and their variants for the formation of UCXBs in the field have been proposed based on the nature of the mass donors, in which the mass donor could be a WD, an evolved main-sequence (MS) star, or a He star (for a review see Nelemans & Jonker 2010).[3] In the classical channel, a NS accretes matter from a WD through RLOF, in which the WD fills its Roche lobe due to the rapid orbital shrinkage induced by GW radiation, known as the WD donor channel (see e.g. Pringle & Webbink 1975; Tutukov & Yungelson 1993; Iben, Tutukov & Yungelson 1995; Yungelson, Nelemans & van den Heuvel 2002; Belczynski & Taam 2004; van Haaften et al. 2012a; Jiang, Chen & Li 2017; Yu, Lu & Jeffery 2021). Sengar et al. (2017) performed a number of complete binary computations for the formation of UCXBs through stable mass transfer from He WDs to NSs, and suggested that this channel can account for the properties of the observed UCXBs with high helium abundances. Bobrick, Davies & Church (2017) recently argued that only binaries containing He WDs with masses less than $0.2\,M_{\odot}$ can undergo stable mass transfer and then form UCXBs. By using a newly suggested magnetic braking prescription from Van, Ivanova & Heinke (2019), Chen et al. (2021) recently found that the initial orbital period range of LMXBs forming UCXBs becomes significantly wider. It has been suggested that at least 100 UCXBs will be detected by *LISA* in the Galaxy based on the WD donor channel (see Tauris 2018).

Podsiadlowski, Rappaport & Pfahl (2002) suggested that LMXBs consisting of a NS and an evolved MS donor with the initial orbital periods below the bifurcation period can also evolve into UCXBs, known as the MS donor channel.[4] van der Sluys, Verbunt & Pols (2005a,b) carried out a number of complete binary computations for this channel, and explored the bifurcation period of LMXBs that can evolve to UCXBs. It has been suggested that the bifurcation period is sensitive to the angular momentum loss mechanisms, especially the magnetic braking laws and the mass-loss prescriptions (see e.g. Ergma 1996; Podsiadlowski, Rappaport & Pfahl 2002; Ma & Li 2009a; Shao & Li 2015; Chen et al. 2017; Deng et al. 2021). It is worth noting that part of the current LMXBs may originate from the evolution of intermediate-mass X-ray binaries (IMXBs) that appear as LMXBs in most of their X-ray active lifetime (e.g. Li 2002, 2015; Podsiadlowski, Rappaport & Pfahl 2002; Xu & Li 2007; Lin et al. 2011; Shao & Li 2012). Chen & Podsiadlowski (2016) argued that the pre-IMXBs with initial orbital periods much near the bifurcation period can evolve towards UCXBs via the magnetic braking caused by the coupling between the magnetic field and an irradiation-driven wind. Chen, Liu & Wang (2020, hereafter Paper I) recently suggested that pre-LMXB/IMXB systems need fine-tuning in the initial orbital period (much near the bifurcation period) to produce detached pre-UCXBs (see also Istrate, Tauris & Langer 2014). In addition, as a variant of the MS donor channel, Ma & Li (2009b) proposed an alternative channel for the formation of UCXBs by considering circumbinary disc-driven mass-transfer.

A NS can also accrete matter from a non-degenerate He star via RLOF, where the mass transfer is driven by GW radiation, known as the He star donor channel (see Savonije, de Kool & van den Heuvel 1986; Heinke et al. 2013). Savonije, de Kool & van den Heuvel (1986) first calculated the evolution of an ultracompact binary with a He star donor, and confirmed that NSs can indeed be accompanied by low-mass He stars. Heinke et al. (2013) argued that the He star donor channel may account for the formation of three persistent UCXBs with relatively long orbital periods (40–60 min) and high mass-transfer rates, but they did not perform complete binary computations. By using a binary population synthesis (BPS) approach, Zhu, Lü & Wang (2012) roughly estimated that about 50 per cent−80 per cent of UCXBs have naked He star donors. However, the parameter space and the rate for the production of UCXBs through this channel are still highly uncertain.

In Paper I, we carried out a systematic study on the detectability of UCXBs by *LISA* through the MS donor channel, and roughly estimated that the number of UCXB-*LISA* sources may reach about 240–320 in the Galaxy. Following the Paper I, the purpose of this paper is to investigate the formation and evolution of UCXBs through the He star donor channel in a systematic way, and then to explore their detectability by *LISA*, *Taiji*, and *TianQin* in the Galaxy. In Section 2, we describe the numerical code and methods for binary evolution calculations. The binary evolutionary results are shown in Section 3. We describe the BPS method and present the corresponding results in Section 4. Finally, a discussion is given in Section 5, and a summary in Section 6.

2 BINARY EVOLUTION CALCULATIONS

In NS+He star systems with tight orbits, GW radiation makes the orbit shrink until the He stars fill their Roche lobes. And then, the He stars start to transfer matter on to the surface of the NSs, resulting in the mass increase of NSs. To investigate the formation of UCXBs through the He star donor channel systematically, it is necessary to carry out detailed binary evolution computations. Employing the stellar evolution code Modules for Experiments in Stellar Astrophysics (MESA, version 12778; see Paxton et al. 2011, 2013, 2015, 2018, 2019), we simulated the long-term evolution of NS+He star systems for the formation of UCXBs. The loss of orbital angular momentum from GW radiation is considered by using a

[2]Another important ultracompact systems are AM CVn binaries, which have similar mass donors with those of UCXBs but the mass-accreting objects are carbon–oxygen (CO) or oxygen–neon (ONe) WDs (see e.g. Warner 1995; Podsiadlowski, Han & Rappaport 2003; Nelemans 2005; Nelemans & Jonker 2010; Solheim 2010; Liu, Jiang & Chen 2021).

[3]In globular clusters, however, the formation of UCXBs is probably dominated by dynamical interactions (e.g. Verbunt 2005).

[4]LMXBs with the initial orbital periods less than the bifurcation period will produce converging systems, otherwise they will form diverging systems (see Pylyser & Savonije 1988, 1989).

standard formula from Landau & Lifshitz (1971),

$$\frac{\mathrm{d}\ln J_{\rm GW}}{\mathrm{d}t} = -\frac{32G^3}{5c^5}\frac{M_{\rm NS}M_2(M_{\rm NS}+M_2)}{a^4}, \quad (1)$$

where $M_{\rm NS}$, M_2, a, G, and c are the mass of the NS, the mass of the He star donor, the orbital separation of the binary, the gravitational constant, and the vacuum speed of light, respectively.

In our simulations, we constructed a grid of binary models for a typical Population I (Pop I) metallicity $Z = 0.02$, in which the He star models are composed of 98 per cent helium and 2 per cent metallicity. For the He star models, we built He stars with zero-age through MESA in idealized methods, in which we neglect all nuclear reactions during their formation, leading to uniform elemental abundance profile from the inside out (see also Wong & Schwab 2019). In particular, more realistic stripped He stars (e.g. hot subdwarf O/B/A stars, horizontal branch stars, etc.) usually have some amount of hydrogen on their surfaces, which makes such stars bigger. The effect of hydrogen in mass transferring from He stars was recently discussed in Bauer & Kupfer (2021).

During the binary evolution, the He star donor transfers some of its matter and angular momentum to the NS once it fills its Roche lobe. Instead of solving the stellar structure equations of NSs, we set the NSs as point masses and adopt the prescription of Tauris & van den Heuvel (2006) for the mass-transfer efficiency with $\alpha = 0$, $\beta = 0.5$, and $\delta = 0$, in which α, β, and δ are the fractions of the mass loss from the vicinity of the He star donor in the form of the stellar wind, the mass loss from the vicinity of the NS, and the circumbinary coplanar toroid, respectively.[5] Accordingly, we define the mass-accretion rate ($\dot{M}_{\rm acc}$) on to the NS as $\dot{M}_{\rm acc} = (1-\beta)\dot{M}_2$, where $\dot{M}_2$ is the mass-transfer rate. If $\dot{M}_{\rm acc}$ is larger than the Eddington accretion rate ($\dot{M}_{\rm Edd}$), we assume that the unprocessed matter is ejected from the vicinity of the NS, taking away the specific orbital angular momentum of the accreting NS (see also Paper I). For He accretion, we set $\dot{M}_{\rm Edd}$ to be $3\times10^{-8}\,{\rm M}_\odot\,{\rm yr}^{-1}$ (e.g. Dewi et al. 2002; Chen, Li & Xu 2011). It has been suggested that the transient behaviour in X-ray binaries results from the thermal–viscous instability of accretion discs (e.g. King, Kolb & Burderi 1996; Dubus et al. 1999). In this work, we rely on the stability criterion based on the irradiated pure helium discs (see e.g. Lasota, Dubus & Kruk 2008; Heinke et al. 2013).

If the NS+He star systems evolve into UCXBs with orbital periods $P_{\rm orb} \lesssim 1$–2 h, they may potentially be detected by low-frequency GW detectors like *LISA*, *Taiji*, and *TianQin*. Here, we set the critical orbital period of UCXBs to be 1 h (e.g. Nelemans & Jonker 2010). Once the calculated characteristic strain is larger than the *LISA* sensitivity, we assume that the corresponding UCXBs are *LISA* sources. In this paper, similar to previous studies (see Tauris 2018; Chen 2020), we adopted the characteristic strain amplitude of UCXBs based on 4 yr of *LISA* observations, written as

$$h_{\rm c} \approx 2.5\times10^{-20}\left(\frac{M_{\rm chirp}}{{\rm M}_\odot}\right)^{5/3}\left(\frac{f_{\rm GW}}{\rm mHz}\right)^{7/6}\left(\frac{15\,{\rm kpc}}{d}\right), \quad (2)$$

in which d is the distance from the source to the detector, and the GW frequency is defined as $f_{\rm GW} = 2/P_{\rm orb}$, where $P_{\rm orb}$ is the orbital period of the binary. For a simplification, we used a formula related to $f_{\rm GW}$ to describe the chirp mass, expressed as

$$M_{\rm chirp} = \frac{c^3}{G}\left(\frac{5\pi^{-8/3}}{96}f_{\rm GW}^{-11/3}\dot{f}_{\rm GW}\right)^{3/5}, \quad (3)$$

in which $\dot{f}_{\rm GW}$ is the derivative of GW frequency (see Tauris 2018).

In principle, equation (3) can only be applied in a detached binary, in which the orbital angular momentum loss is fully contributed by GW radiation. However, the mass transfer between two components of UCXBs and the mass loss of the system also have influence on the orbital evolution. Therefore, a dynamical chirp mass was defined (see equation 4 in Tauris 2018). Especially, the GW frequency will decrease in the orbit expanding stage, resulting in a negative chirp (e.g. Kremer et al. 2017). It is worth noting that equation (3) is still representative of the chirp mass by order of magnitude since the mass transfer is driven by GW radiation and happens on a time-scale close to that of GWs.

We incorporated the prescriptions above into MESA and evolved a large number of NS+He MS systems for producing UCXBs, thus obtaining a large, dense model grid of binaries. In our simulations, the initial parameter ranges of NS+He star systems were chosen, as follows: (1) the initial masses of the NSs, $M^{\rm i}_{\rm NS}$, are set to be $1.4\,{\rm M}_\odot$; (2) the initial masses of the He star donors, $M^{\rm i}_2$, range from $0.32\,{\rm M}_\odot$ (the minimum mass for a He star to ignite helium in its centre) to $1.20\,{\rm M}_\odot$ (the upper limit on He MS mass for a NS+He MS binary to produce a UCXB in our simulations), where we used an equal step of $\triangle M_2$ to be $0.1\,{\rm M}_\odot$; (3) the initial orbital periods of the binaries, $P^{\rm i}_{\rm orb}$, change from the minimum value (at which a He star with zero-age fills its Roche lobe) to the maximum value (at which the He star fills its Roche lobe when its central He is exhausted), where we set $\triangle\log P_{\rm orb}$ to be 0.1.

3 BINARY EVOLUTION RESULTS

We performed a large number of complete binary evolution computations of NS+He star systems for the formation of UCXBs. Table 1 lists the main evolutionary properties of some typical NS+He star systems that can evolve into UCXBs. In this table, we first mainly explored the effect of different initial He star masses on the final results (see sets 1–5), and then the effect of different initial orbital periods (see sets 6–11).

3.1 A typical example for binary evolution

Fig. 1 shows a typical example of the evolution of a NS+He star system that can form a UCXB (see set 2 in Table 1). The initial parameters for this binary are $(M^{\rm i}_2, M^{\rm i}_{\rm NS}, \log(P^{\rm i}_{\rm orb}/{\rm d})) = (0.40, 1.40, -1.80)$, in which $M^{\rm i}_2$, $M^{\rm i}_{\rm NS}$, and $P^{\rm i}_{\rm orb}$ are the initial mass of the He star and the NS in solar mass, and the initial orbital period in days, respectively. Because of the short initial orbital period, the angular momentum loss induced by the GW radiation is large enough to result in the rapid shrinking of the orbital separation. After about 0.37 Myr, the He star begins to fill its Roche lobe while it is still in the He-core burning stage (case BA mass transfer; see Dewi et al. 2002). After the beginning of the mass transfer, the binary appears to be a persistent UCXB soon. The binary shows as a persistent source lasting for ∼46.6 Myr.

The binary undergoes severe orbital angular momentum loss through GW radiation and thus keeps much higher mass-transfer rates during the UCXB stage. After about 4.15 Myr, the He star decreases its mass to $0.236\,{\rm M}_\odot$ and the binary evolves to the minimum orbital period ($P^{\rm min}_{\rm orb} = 10.47$ min). At this stage, helium

[5]Similar to previous studies (see Podsiadlowski, Rappaport & Pfahl 2002; Paper I), we arbitrarily set β to be 0.5 in this work. We have computed some models with $\beta = 0.7$, and found that the β value has no significant influence on the final results.

Table 1. Selected evolutionary properties of some typical UCXBs with different initial secondary masses and initial orbital periods. The columns (from left to right): the initial mass of the donor star and the initial orbital period; the stellar age at the onset of RLOF; the minimum orbital period, the stellar age, the donor mass, and the GW frequency at the minimum orbital period; the stellar age, the donor mass, the carbon mass fraction at the centre of the donor star, the NS mass, and the orbital period when the binary evolution terminates; the time-scale being a persistent UCXB based on an irradiated pure helium disc; and the time-scale that the binary appears to be as a *LISA* source based on a distance of 15 kpc.

Set	$M_2^{\rm i}$ ($M_\odot$)	$\log P_{\rm orb}^{\rm i}$ (d)	$t_{\rm RLOF}$ (Myr)	$P_{\rm orb}^{\rm min}$ (min)	$t^{\rm min}$ (Myr)	$M_2^{\rm min}$ ($M_\odot$)	f_{LISA} (mHz)	$t^{\rm f}$ (Gyr)	$M_2^{\rm f}$ ($M_\odot$)	$X_{\rm C}^{\rm f}$	$M_{\rm NS}^{\rm f}$ ($M_\odot$)	$P_{\rm orb}^{\rm f}$ (min)	$\triangle t_{\rm per}$ (Myr)	$\triangle t_{LISA}$ (Myr)
1	0.32	−1.90	0.75	8.12	1.06	0.293	4.11	6.60	0.0054	0.008	1.520	73.44	46.1	26.0
2	0.40	−1.80	0.37	10.47	4.15	0.236	3.17	7.27	0.0052	0.012	1.585	74.88	46.6	30.1
3	0.50	−1.65	1.00	10.34	8.27	0.247	3.22	4.72	0.0085	0.065	1.636	66.24	50.0	32.1
4	0.60	−1.55	1.92	10.37	14.22	0.241	3.21	3.21	0.0101	0.170	1.678	63.78	55.7	37.7
5	0.70	−1.50	1.95	10.34	20.45	0.232	3.22	0.02	0.1824	0.294	1.645	11.10	–	–
6	0.40	−1.70	1.71	10.24	5.31	0.242	3.25	8.91	0.0049	0.022	1.581	77.89	48.1	31.1
7	0.40	−1.60	4.27	10.24	7.94	0.241	3.25	3.97	0.0091	0.040	1.579	62.19	48.7	31.4
8	0.40	−1.50	8.99	10.12	12.72	0.242	3.29	4.61	0.0087	0.070	1.578	66.82	53.2	36.0
9	0.40	−1.40	17.74	10.05	21.59	0.243	3.32	3.96	0.0094	0.124	1.577	65.39	62.6	38.3
10	0.40	−1.30	33.87	10.19	37.97	0.245	3.27	2.57	0.0112	0.199	1.578	61.23	79.8	38.6
11	0.40	−1.20	63.41	10.34	68.48	0.233	3.22	0.07	0.0953	0.346	1.541	16.47	–	–

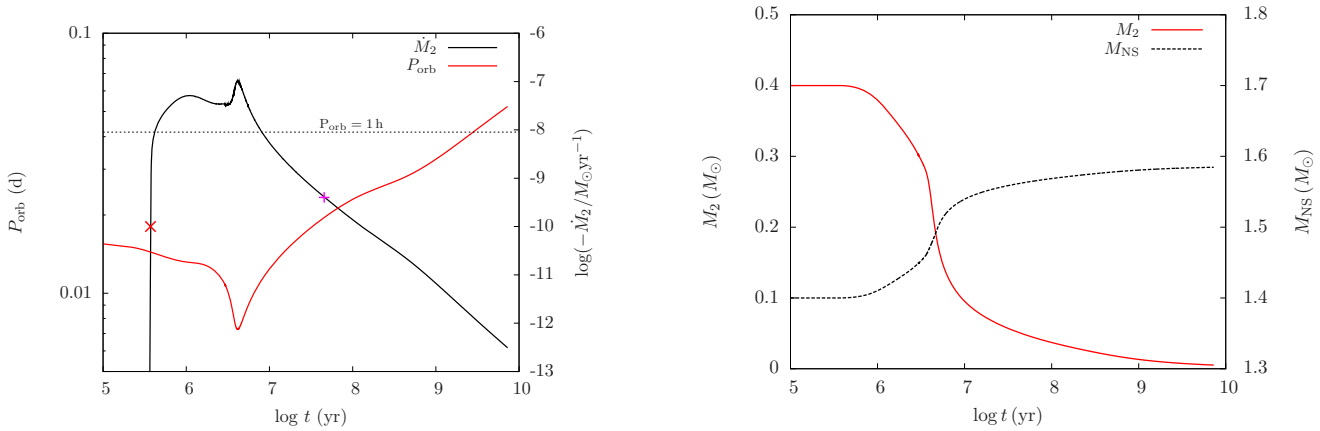

Figure 1. A representative example of the evolution of a NS+He star system that can form a UCXB, where $(M_2^{\rm i}, M_{\rm NS}^{\rm i}, \log(P_{\rm orb}^{\rm i}/{\rm d})) = (0.40, 1.40, -1.80)$ (see set 2 in Table 1). Left-hand panel: the evolution of binary orbital period (red solid curve, left-hand axis) and the mass-transfer rate (black solid curve, right-hand axis) as a function of time for the binary evolution calculations. The red cross indicates the starting point as a persistent UCXB, whereas the pink plus represents the end point as a persistent source. The horizontal black dotted line shows a critical orbital period of 1 h. Right-hand panel: the evolution of the mass of the He star donor (red solid curve, left-hand axis) and the mass of the NS (black dashed curve, right-hand axis) as a function of time.

burning in the centre of the He star starts to fade. After that, the binary orbit starts to expand, and the mass-transfer rate begins to decrease (for more discussions see Section 3.2). The binary appears to be a UCXB lasting for about 2.8 Gyr based on a critical orbital period of 1 h. When the He star donor decreases its mass to 0.0052 $M_\odot$, the evolutionary code stops because of hitting the equation-of-state (EOS) limits (max_log $Q > 5$; a MESA default value), where $\log Q = -2\log T + \log\rho + 12$, in which T and ρ are the temperature and density in a specific zone of the star, respectively. At this moment, the lifetime of the binary is 7.27 Gyr, the mass of the NS is $M_{\rm NS}^{\rm f} = 1.585\,M_\odot$, and the orbital period is $P_{\rm orb}^{\rm f} = 74.88$ min.

3.2 Evolutionary tracks of UCXBs

Fig. 2 presents the evolutionary tracks of five typical UCXBs with different initial He star masses (see sets 1–5 in Table 1) in the orbital period versus the secondary mass diagram. These NS+He star systems would directly evolve into UCXBs once the He star donors fill their Roche lobes. During the UCXB stage, the angular momentum loss is dominated by GW radiation. When the masses of the He star donors drop below ∼0.3 $M_\odot$, the minimum orbital periods of these binaries will be approached soon. The minimum orbital periods of UCXBs in this work are in the range of 8–10 min, which are larger than those in NS+He WD systems a little bit (5–7 min; see e.g. Sengar et al. 2017; Paper I). The main reason is that He WDs are more compact than He star donors. At the stage of the minimum orbital periods, helium burning in the centre of the He star donors is gradually extinguished. Meanwhile, the He star donors gradually reach a state of mildly degenerate, indicating that their mass–radius exponent is negative.

In Fig. 2, we note that the NS+He star system with $M_2^{\rm i} = 0.32\,M_\odot$ has a lower minimum orbital period. This is because the system contains a slightly more massive donor at the moment of the minimum orbital period (see Table 1), which is more compact than that of a less massive one for degenerate stars. With the evolution of the UCXBs, the masses of the donors and the mass-transfer rates become lower and lower after the minimum orbital periods (see Fig. 3). Meanwhile, the binary orbits gradually widen (see Fig. 2),

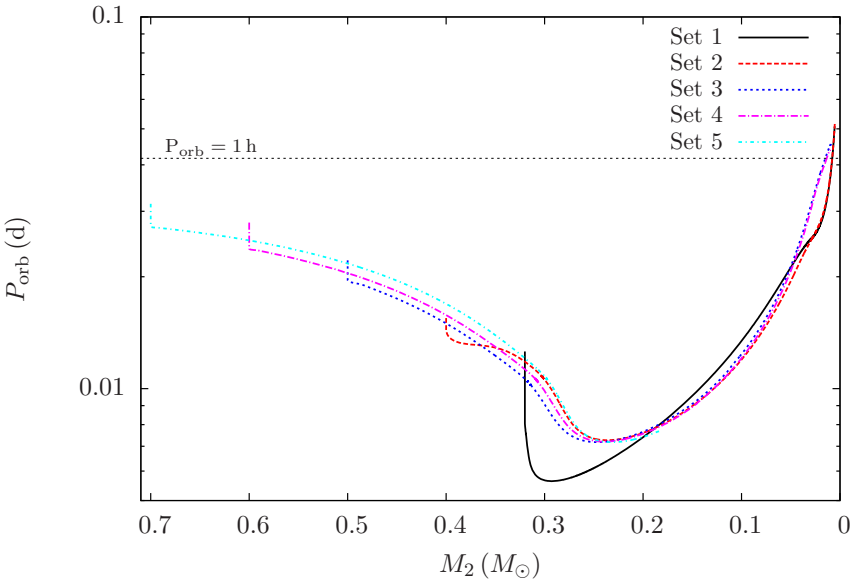

Figure 2. Evolutionary tracks of five typical UCXBs with different initial He star masses (see sets 1–5 in Table 1) in the orbital period versus the secondary mass diagram, where the horizontal black dotted line shows a critical orbital period of 1 h.

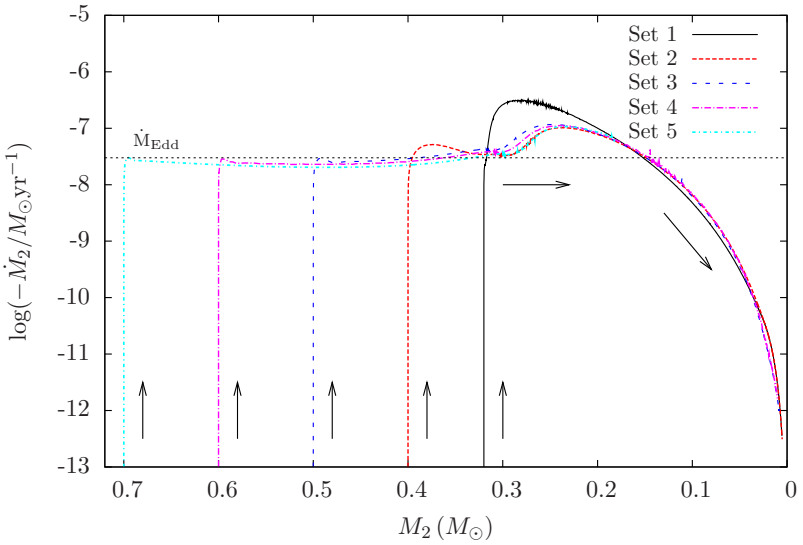

Figure 3. Evolutionary tracks of five typical UCXBs with different initial He star masses (see sets 1–5 in Table 1) in the mass-transfer rate versus the secondary mass diagram, where the tracks follow the direction of the black arrows. The dotted line is $\dot{M}_{\rm Edd}$ for a NS that is accreting He-rich material.

resulting from the mass and radius relation for degenerate mass donors whereby they expand in response to mass loss (see also Savonije, de Kool & van den Heuvel 1986; Sengar et al. 2017). These binaries appear to be UCXBs lasting for about 1.5–4.0 Gyr, where they present as persistent sources with lifetime about 40–80 Myr. Note that the NS+He star system represented by set 5 quickly enters into the mass-transfer stage due to the short orbital period, leading to the formation of a UCXB. After about 20.45 Myr, as shown in Fig. 2, the binary enters into the minimum orbital period, after which we suffer from some numerical difficulties for the evolution of the NS system (for a similar case, see set 11 in Table 1).

After the UCXB stage, the evolved NS systems will form millisecond radio pulsars, in which the pulsars have been regenerated by mass-accretion-induced spin-up. If the millisecond pulsars start to evaporate their companions, Black Widows will be formed (see e.g. van den Heuvel & van Paradijs 1988; Ruderman, Shaham & Tavani 1989; Chen et al. 2013; Tang & Li 2021). The NS systems studied here will eventually produce single millisecond radio pulsars or pulsar+planet-like systems (for more discussions see Section 5).

3.3 The $\dot{M}_2$–$P_{\rm orb}$ diagram

Fig. 4 represents the evolutionary tracks of four typical UCXBs with different initial He star masses (see sets 1–4 in Table 1) in the mass-transfer rate versus the orbital period diagram. The evolutionary tracks in this diagram exist two stages (see also Sengar et al. 2017),

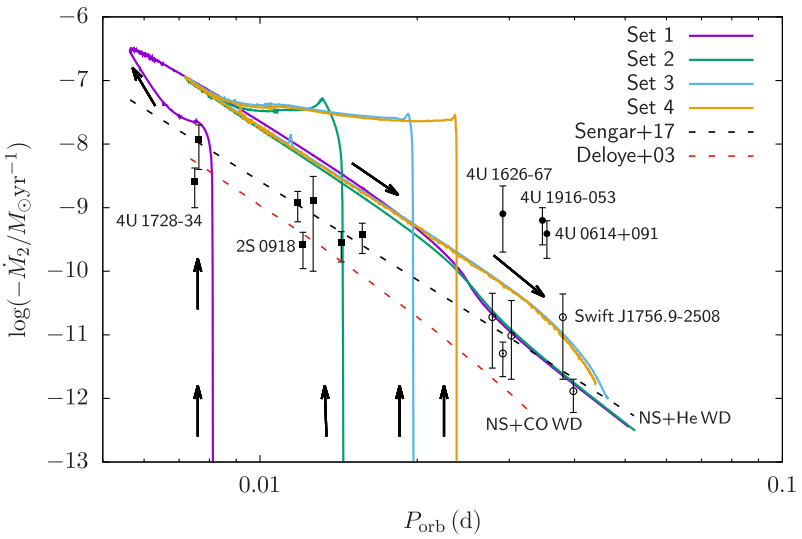

Figure 4. Evolutionary tracks of four typical UCXBs with different initial He star masses (see sets 1–4 in Table 1) in the mass-transfer rate versus the orbital period diagram, where the tracks follow the direction of the black arrows. For a comparison, in this figure we also plot the theoretical evolutionary tracks of the mass-transfer rates on the declining stage based on the NS+He WD channel and the NS+CO WD channel. The black dashed line shows the numerical relation fit between the mass-transfer rate and the orbital period based on the NS+He WD channel (see Sengar et al. 2017), whereas the red dashed line presents the low-entropy evolutionary tracks for degenerate O donors based on the NS+CO WD channel (see Deloye & Bildsten 2003). More details of the orbital period and the mass-transfer rate changing with the secondary mass can be found in Figs 2 and 3. The solid squares, solid circles, and open circles denote seven persistent sources with short orbital periods, three persistent sources and five transient sources with relatively long orbital periods (40–60 min), respectively. The observational data are taken from Heinke et al. (2013). Note that the upper and lower error estimates for the mass-transfer rates are still not well determined, and the orbital periods of two UCXBs (i.e. 4U 1728−34 and 4U 0614+091) may not be correct in these observational data (see Heinke et al. 2013).

as follows. (1) *The ascending stage*. The orbital periods continue to decrease due to GW radiation after the He star donors fill their Roche lobes, whereas the tracks of the mass-transfer rates enter into the ascending stage until the tip at the minimum orbital periods. (2) *The declining stage*. Following the minimum orbital periods, the tracks of the mass-transfer rates get into the declining stage, while the orbital periods increase. The observed UCXBs are much more likely to be on the declining stage as their evolutionary lifetime is much longer than a Gyr along this stage (see also Deloye & Bildsten 2003; Nelemans et al. 2010; Sengar et al. 2017).

As shown in Fig. 4, our UCXB tracks can explain the location of the five transient sources with relatively long orbital periods quite well, especially for Swift J1756.9−2508 that cannot be reproduced by the WD donor channel. For a comparison, in this figure we also plot the numerical relation fit between the mass-transfer rate and the orbital period based on the NS+He WD channel (see Sengar et al. 2017) and the low-entropy evolutionary tracks for degenerate O donors based on the NS+CO WD channel (see Deloye & Bildsten 2003). We note that most of UCXBs are consistent with the evolutionary tracks of the NS+He WD channel. Meanwhile, one UCXB (2S 0918−549) can be reproduced by a low-entropy CO WD donor, consistent with carbon and oxygen lines in its optical spectra (see Deloye & Bildsten 2003).

However, three persistent sources that have relatively long orbital periods (40–60 min) and high mass-transfer rates ($>10^{-10}\,\mathrm{M}_\odot\,\mathrm{yr}^{-1}$) are inconsistent with the tracks of the WD donor channel (see also Heinke et al. 2013). In the three persistent sources, one UCXB (4U 1916−053) exhibits strong helium lines in its optical spectra (probably containing a He star donor; e.g. Nelemans, Jonker & Steeghs 2006), and two UCXBs (4U 1626−67 and 4U 0614+091) clearly show the lack of hydrogen and helium lines but present carbon and oxygen lines in their optical spectra (likely having CO WD donors; see e.g. Nelemans et al. 2004, 2006; Werner et al. 2006). In this work, the ascending stage of massive He star donors could pass near 4U 1916−053, but the passage time through that region is too short. The descending stage instead goes too far below the three persistent sources (see Fig. 4). It has been argued that 4U 1626−67 was produced through accretion-induced collapse of a ONe WD accretor, likely containing a neon-enriched donor (see Yungelson, Nelemans & van den Heuvel 2002). For more discussions on the formation of the three persistent sources, see Section 5.

In Fig. 4, we note that the mass-transfer rates on the declining stage have a bifurcation after $P_{\rm orb} > 0.02$ d through the He star donor channel, where the mass donors become lower than $0.06\,\mathrm{M}_\odot$. This bifurcation also appears for the cases with different initial orbital periods (see Fig. 5). Fig. 6 shows the evolutionary tracks of UCXB donor stars for $M_2^{\rm i} = 0.40\,\mathrm{M}_\odot$ with different initial orbital periods in the central temperature versus the central mass density diagram. As shown in this figure, the bifurcation may be mainly caused by the central temperature of the mass donors; a mass donor with higher central temperature (higher central carbon mass fraction) has lower degeneracy, resulting in higher mass-transfer rates on the declining stage.

3.4 Gravitational wave signals

The observation of GW radiation has started a new astronomical era after the detection of high-frequency GW signals from the first double BH coalescence event (GW150914) by the ground-based Advanced Laser Interferometer Gravitational-Wave Observatory (aLIGO)/Virgo (see Abbott et al. 2016). The second historic moment is the GW detection of the first double NS coalescence event (GW170817) together with the entire electromagnetic

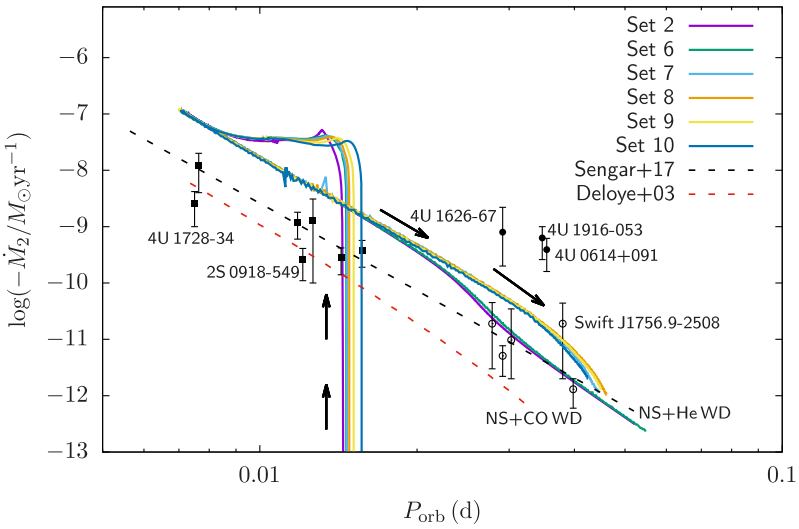

Figure 5. Similar to Fig. 4, but for the evolutionary tracks of UCXBs for $M_2^{\rm i} = 0.40\,{\rm M}_\odot$ with different initial orbital periods (see sets 2 and 6–10 in Table 1).

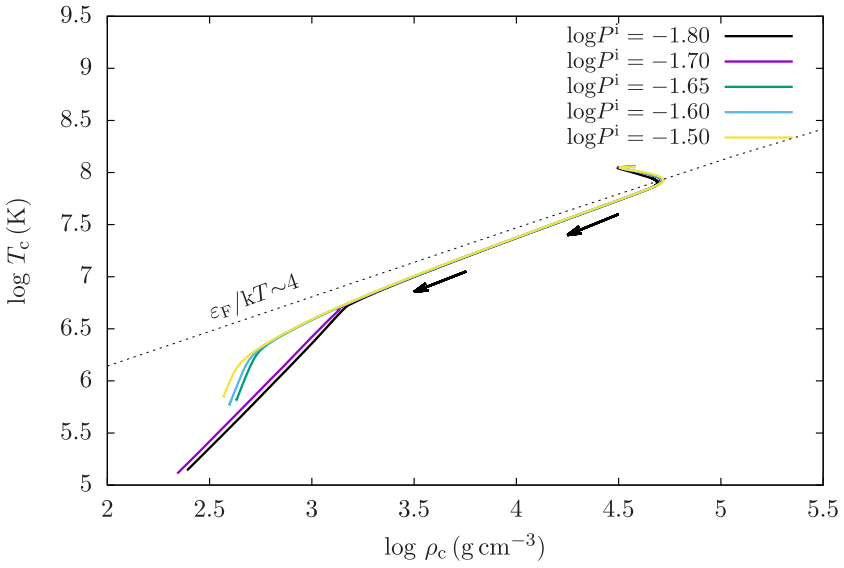

Figure 6. Evolutionary tracks of UCXB donor stars for $M_2^{\rm i} = 0.40\,{\rm M}_\odot$ with different initial orbital periods in the central temperature versus the central density diagram, where the tracks follow the direction of the black arrows. Non-degenerate and degenerate regions are separated by the dotted line ($\varepsilon_{\rm F}/kT \sim 4$).

spectrum from gamma-rays to radio signals, becoming a milestone in multimessenger astrophysics (see Abbott et al. 2017). UCXBs have been thought to be the potential GW sources in the low-frequency region, which would be observable by the future space-based GW observatories like *LISA*, *Taiji*, and *TianQin*. Owing to the continuous mass accretion, they provide a favourable advantage to carry out full multimessenger investigations in both electromagnetic spectrum and GW signals.

Fig. 7 shows the evolutionary tracks of four typical UCXBs with different initial He star masses (see sets 1–4 in Table 1) in the characteristic strain amplitude versus the GW frequency diagram. We suppose that a UCXB can be visible as a *LISA* source once the calculated characteristic strain is larger than the *LISA* sensitivity. Note that this assumption only provides an upper limit for the number estimation of UCXB-*LISA* sources. From this figure, we can see that UCXBs through the He star donor channel can be detected by the future space-based GW observatories like *LISA*, *Taiji*, and *TianQin*. Because of the short initial orbital periods, the preceding detached NS+He star binaries will be also detected by the GW observatories and would be observable as binary radio pulsars. Meanwhile, the sources will be both seen as persistent UCXBs and GW sources simultaneously after the onset of the mass transfer.

With the evolution of a UCXB, the peak characteristic strain approaches when the minimum orbital period is coming. In our simulations, all NS+He star systems forming UCXBs can be detectable by *LISA* within a distance of 15 kpc. At distances up to the edge of the Galaxy (∼100 kpc), they are even be visible as *LISA* sources. The average $\triangle t_{LISA}$ within a distance of 15 kpc is about

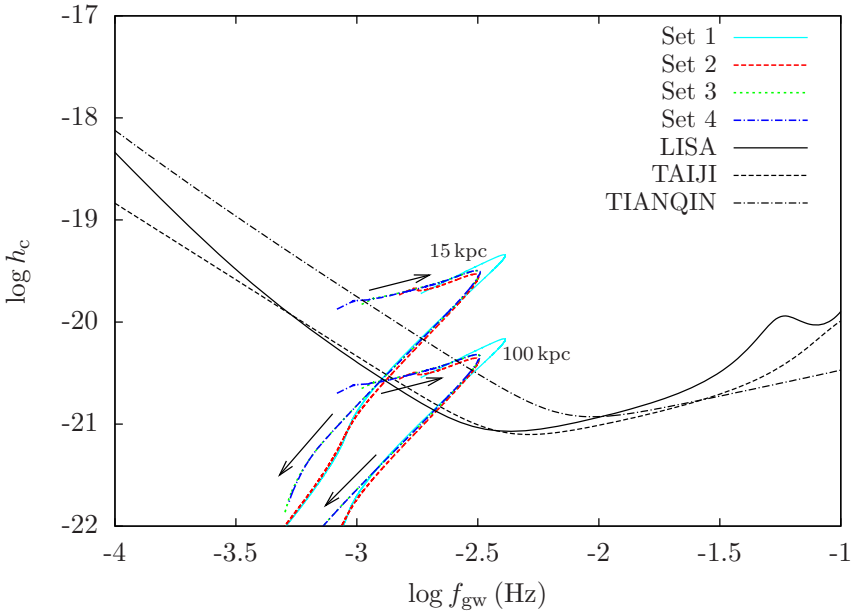

Figure 7. Evolutionary tracks of four typical UCXBs with different initial He star masses (see sets 1–4 in Table 1) in the characteristic strain amplitude versus the GW frequency diagram, where the tracks follow the direction of the black arrows. The upper and lower curves represent the binary evolution results based on the distance of 15 and 100 kpc from the source to the detectors, respectively. The sensitivity curve for the future space-based GW observatory *LISA* is from the numerical calculations based on 4 yr of observations (see Robson, Cornish & Liu 2019). For comparison, in this figure we also present the *Taiji* sensitivity curve (see Ruan et al. 2020) and the *TianQin* sensitivity curve (see Wang et al. 2019).

33 Myr in our simulations (see Table 1). We also note that most of UCXBs produced by the MS donor channel can only be visible by *LISA* within a distance of 1 kpc (see Paper I). Compared with the MS donor channel, UCXBs from the He star donor channel are easier to be discovered by *LISA*.

3.5 Initial parameters of NS+He star systems

We evolved a large number of NS+He star systems for the formation of UCXBs, and thereby obtained a large, dense model grid of binaries. Fig. 8 presents the initial contour for producing UCXBs in the log $P^{\rm i}$–$M_2^{\rm i}$ plane, where $P^{\rm i}$ and $M_2^{\rm i}$ are the initial orbital period and the initial mass of the He star donor, respectively. If the initial parameters of a NS+He star system are located in the contours, a UCXB is then supposed to be formed. Thus, the contours can be expediently used in BPS simulations to study the formation of UCXBs. In our calculations, the estimated minimum orbital periods of UCXBs with He star donors are close to 8 min (see set 1 in Fig. 2). We also found that NS+He star systems initialized at wider orbits and coming into contact due to GW radiation would also be observed as UCXBs (see also Fig. 5). Note that all UCXBs in this contour can be visible as *LISA* sources within a distance of 15 kpc, and they will be still detectable as *LISA* sources within a distance of 100 kpc.

The initial parameter space for producing UCXBs is constrained by the following conditions. (1) The left-hand boundary of the contour is set by the condition that RLOF starts when the He star is on the zero-age MS stage. (2) The lower boundary is constrained by the requirements that the masses of He stars in close binaries should be larger than 0.32 $M_\odot$, below which helium burning in their centre would be extinguished (see also Han et al. 2002; Yungelson 2008). (3) The systems beyond the right-hand boundary start mass transfer when the He stars are on the subgiant stage and have CO cores. Note that systems close to the right-hand boundary can also form UCXBs when the He stars evolve to the subgiant stage, but we did not consider this case in this work.

4 BPS ASSUMPTIONS AND RESULTS

4.1 BPS assumptions

To investigate the Galactic rates of UCXBs through the He star donor channel, a series of Monte Carlo BPS simulations is carried out based on the rapid binary star evolution (BSE) code developed by Hurley, Tout & Pols (2002). The principal assumptions and basic BPS set-up in this work are similar to those in Paper I, but here we adopted the updated initial parameter space of the He star donor channel for producing UCXBs. In the BPS approach, the primordial binary samples are obtained in the way of Monte Carlo simulations. In each simulation, a sample of 1×10^7 primordial binaries is tracked until the formation of NS+He star systems. We assume that a UCXB would be formed when the initial parameters of a NS+He star system are located in the UCXB parameter space of Fig. 8. Note that the He stars from the BSE code here are identified with He stars initialized in MESA simulations.

NS+He star systems for producing UCXBs have most likely emerged from the common-envelope (CE) evolution of giant binaries as they have ultrashort orbital periods. We assume that the mass transfer would be dynamically unstable and a CE would be formed when the mass ratio of the binary is larger than a critical value ($q_{\rm c}$; see Paczyński 1976). It has been generally thought that $q_{\rm c}$ changes with the evolutionary stage of the primordial primary once it fills its Roche lobe (e.g. Hjellming & Webbink 1987; Han et al. 2002; Podsiadlowski, Rappaport & Pfahl 2002). In this work, we set $q_{\rm c} = 4$ once the primary is in the MS or Hertzsprung gap stage (e.g. Han, Tout & Eggleton 2000; Chen & Han 2003). When the mass donor is a red giant (RG) star or an asymptotic giant branch (AGB) star, we

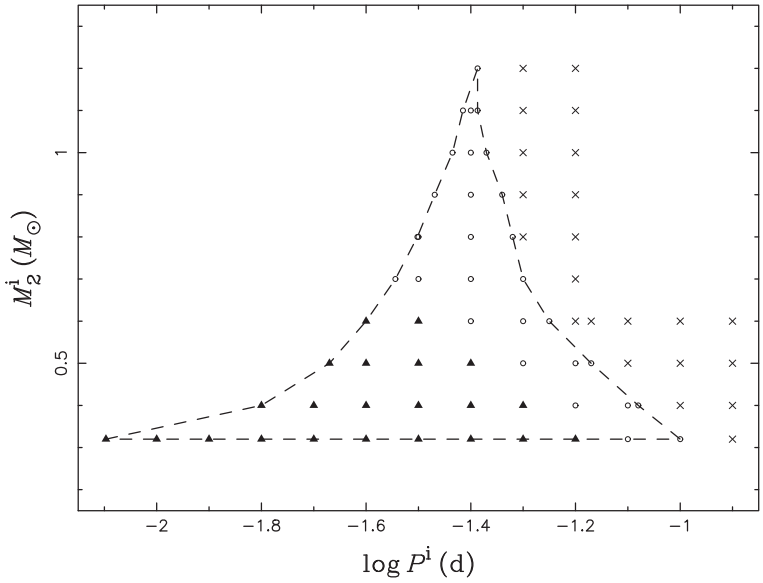

Figure 8. Regions in the initial orbital period–secondary mass plane ($\log P^i$, M_2^i) for NS+He star binaries that can produce UCXBs, in which the initial mass of NSs is assumed to be 1.4 $M_\odot$. The filled triangles and open circles stand for the binaries resulting in the formation of UCXBs. For the binaries represented by the filled triangles, the evolutionary code terminates because of hitting EOS limits. For the binaries marked by the open circles, the evolutionary code stops due to the numerical difficulties we suffered after the minimum orbital period (e.g. set 5 in Fig. 2). Crosses are for those that the He star fills its Roche lobe when it evolves to the subgiant stage.

adopt

$$q_c = \left[1.67 - x + 2\left(\frac{M_{c1}}{M_1}\right)^5\right] \Big/ 2.13, \quad (4)$$

where M_{c1}, M_1, and $x = \mathrm{d}\ln R_1/\mathrm{d}\ln M_1$ are the core mass of the donor, the donor mass, and the mass–radius exponent of the donor, respectively (see Hurley, Tout & Pols 2002).

The CE ejection process is still highly uncertain (e.g. Ivanova et al. 2013; Soker 2013; Soker, Grichener & Sabach 2018; Kruckow et al. 2021). As in our previous studies (see Wang et al. 2009), the standard energy prescription is adopted to calculate the CE evolution (see Webbink 1984), in which we combine the CE ejection efficiency (α_{CE}) and the stellar structure parameter (λ) into a free parameter $\alpha_{CE}\lambda$ and set it to be 1.0 as our standard model. Note that other energy sources (e.g. the internal energy of the envelope) may also contribute to the CE ejection (see Han, Podsiadlowski & Eggleton 1995). Thus, we consider the effect of a larger value of $\alpha_{CE}\lambda$ (i.e. 1.5) on the final results for a comparison.

The following input is adopted in our BPS Monte Carlo simulations (for a recent review see Han et al. 2020; see also Han 2008; Wang, Podsiadlowski & Han 2017). (1) We used the initial mass function from Miller & Scalo (1979). (2) All stars are assumed to be members of binaries, and a constant mass-ratio distribution is adopted. (3) A circular orbit is supposed for the primordial binaries. (4) The orbital separation distribution is supposed to be constant in $\log a$ for wide primordial binaries, in which a is the orbital separation of the binary. (5) A constant star formation rate (SFR) is assumed over the past 15 Gyr, in which we suppose that a primordial binary with its primary $> 0.8\,M_\odot$ is produced every year (see Han, Podsiadlowski & Eggleton 1995; Hurley, Tout & Pols 2002). From this calibration, a constant SFR of $5\,M_\odot\,\mathrm{yr}^{-1}$ can be obtained (see Willems & Kolb 2004).

4.2 BPS results

Fig. 9 shows the evolution of the Galactic rates of UCXBs for the He star donor channel by adopting a constant Pop I SFR of $5\,M_\odot\,\mathrm{yr}^{-1}$. The simulations give the theoretical rates of He star UCXBs in the Galaxy to be $\sim$3.1–11.9 Myr^{-1}. If we adopt the time-scale of UCXBs appearing as *LISA* sources to be 33 Myr within a distance of 15 kpc (see Table 1), there exist about 100–390 UCXB-*LISA* sources in the Galaxy, at least providing an upper limit for their number estimation. This work indicates that the He star donor channel has significant contribution to the formation of UCXBs.

It is worth noting that there are about six persistent UCXBs in the field (e.g. Heinke et al. 2013). Persistent UCXBs are believed to be detectable in the whole Galaxy, which have lifetimes of about 30–100 Myr (e.g. Tauris 2018; Paper I). Thus, the empirical observed formation rates for persistent UCXBs are about $6/(30\text{–}100) = (0.06\text{–}0.2)\,\mathrm{Myr}^{-1}$. The theoretical UCXB rates for the He star donor channel are about 15–200 times larger than the observational values. Accordingly, calibrating by the UCXB observations, we roughly estimate that the expected number for such UCXB-*LISA* sources in the Galaxy is about 1–26 (calculated here as 100/200–390/15).

It seems that the theoretical UCXB rates from the He star donor channel are far more above the observed rates. The main reason for such a discrepancy is due to some uncertainties in our BPS simulations, as follows. (1) Other Galactic models have already predicted several times smaller SFRs. For example, Licquia & Newman (2014) recently suggested a lower Galactic SFR of $1.66\,M_\odot\,\mathrm{yr}^{-1}$ based on a hierarchical Bayesian statistical analysis. If this SFR is adopted, the theoretical UCXB rates will decrease to be $\sim 1.0\text{–}4.0 \times 10^{-6}\,\mathrm{yr}^{-1}$ in the Galaxy. (2) Recent simulations imply that the critical mass ratio (i.e. the stability criteria) for RG/AGB mass transfer is likely to be larger than the adopted value here (e.g. Ge et al. 2020). This indicates that we may slightly overestimate the rates of NS+He star systems.

As shown in Fig. 9, there exist two obvious ascending stages for the evolution of UCXB rates, i.e. with the delay time around 100 and

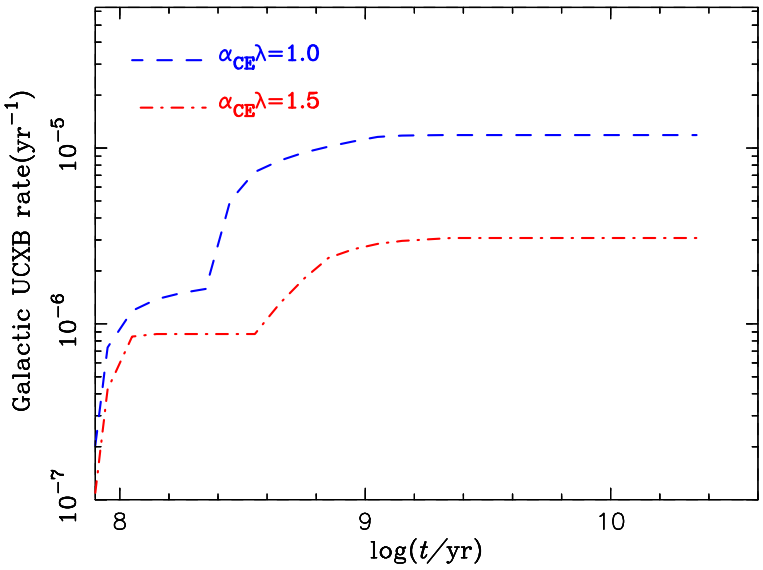

Figure 9. Evolution of the Galactic rates of UCXBs from the He star donor channel as a function of time by adopting a constant Population I (Pop I) SFR of $5\,M_{\odot}\,yr^{-1}$.

300 Myr from the star formation to the formation of UCXBs. These two cases correspond to two specific evolutionary scenarios for the formation of NS+He star systems, in which the primordial primaries (i.e. the progenitors of NSs) first fill their Roche lobes and then form CEs (1) at the RG stage for the case with short delay times and (2) at the AGB stage for the case with long delay times. For scenario (1), the initial parameters of the primordial binaries are in the range of $M_{1,i} \sim 10$–$25\,M_{\odot}$, $q = M_{2,i}/M_{1,i} \sim 0.1$–$0.3$, and $P^{i} \sim 20$–2000 d, in which $M_{1,i}$, $M_{2,i}$, P^{i}, and q are the initial masses of the primordial primary and secondary, the initial orbital period, and mass ratio of the primordial systems, respectively. About 15 per cent of UCXBs from the He star donor channel are produced through this scenario. For scenario (2), the initial parameters of the primordial binaries are in the range of $M_{1,i} \sim 7$–$15\,M_{\odot}$, $q \sim 0.2$–0.8, and $P^{i} \sim 600$–4000 d. About 85 per cent of UCXBs from the He star donor channel are formed through this scenario.

5 DISCUSSION

It has been argued that the He star donor channel may produce higher average mass-transfer rates in the three persistent UCXBs with relatively long orbital periods if the He star donors can retain their initial high entropy (see Heinke et al. 2013). In this work, we found that a He star donor with higher central temperature (higher central carbon mass fraction) has lower degeneracy, corresponding to higher mass-transfer rates on the declining stage. Note that we did not consider the irradiation effect of X-ray luminosities of mass-accreting NSs on the evolution of UCXBs, which may also trigger higher mass-transfer rates (see e.g. van Haaften et al. 2012c; Jia & Li 2015; Lü et al. 2017). Thus, we speculate that the He star donor channel has the potential ability to account for the formation of the three persistent sources with higher mass-transfer rates, especially for 4U 1916−053 that probably has a He star donor. If the three persistent sources really originate from the He star donor channel, we expect the initial He star mass larger than $0.6\,M_{\odot}$. In this work, we suffer from some numerical difficulties for the evolution of NS systems with the central carbon abundances of the mass donors higher than 20 per cent when the binary orbits gradually widen (see e.g. set 5 in Fig. 2). Complete binary computations on these systems are encouraged to unveil the origin of the three persistent sources.

As shown in Fig. 4, different channels for the formation of UCXBs predict distinct mass-transfer rates on the declining stage owing to different degeneracy for mass donors; the mass donors with lower degeneracy correspond to higher mass-transfer rates on the declining stage. Thus, we emphasize that the relation in the diagram between the mass-transfer rate on the declining stage and the orbital period can be used to distinguish the mass donors in UCXBs. Meanwhile, different UCXB formation channels have different mass-donor chemical compositions, which can be used to provide support for the mass-donor identifications (e.g. Koliopanos et al. 2021). Hence, more observations on the chemical compositions of the mass donors in UCXBs are needed.

For the three formation channels of UCXBs, the total UCXB lifetime is mainly determined by the initial orbital periods of pre-UCXB systems. If we set the critical orbital period of UCXBs to be 1 h, the total UCXB lifetime is about 2–4 Gyr; we found that the total UCXB lifetime is no big difference for the three channels (see also Tauris 2018; Paper I). In addition, persistent UCXBs from the He star donor channel have lifetimes of 40–80 Myr, which are shorter than those from the MS donor channel (50–150 Myr; see Paper I), but longer than those from the He WD donor channel (20–40 Myr; e.g. Tauris 2018). Furthermore, compared with the WD/MS donor channels, the He star donor channel has higher possibility to form millisecond radio pulsars as their typical delay times from the star formation to the formation of UCXBs are shorter than those from the WD/MS donor channels.

In this work, the He star donors can decrease their masses to $\sim 0.005\,M_{\odot}$ when the binary evolution terminates because of hitting EOS limits. Ruderman & Shaham (1985) suggested that NSs will tidally disrupt the very low mass He degenerate donors before they decrease to $0.004\,M_{\odot}$ as the mass donors change their mass–radius relation, eventually forming single millisecond pulsars. We also note that the NS+He star systems have the potential possibilities to leave behind pulsar+planet-like systems at the end of their evolution (e.g. Podsiadlowski 1993). Pulsar timing observations have revealed three pulsar+planet-like systems so far, in which all planet-like objects are

around old millisecond pulsars (e.g. Martin, Livio & Palaniswamy 2016). Especially, Bailes et al. (2011) reported a planet-like object around the millisecond pulsar PSR J1719−1438, and suggested that this system may have once been a UCXB, in which the mass donor narrowly avoided complete destruction (see also van Haaften et al. 2012b).

UCXBs are important continuous GW sources in the low-frequency region. Some recent studies carried out systematic studies on the detectability of UCXBs by *LISA* through the WD/MS donor channels, and suggested that several hundred UCXB-*LISA* sources would be detected in the Galaxy (see Tauris 2018; Paper I). In this work, the preceding detached NS+He star systems can be detected by the GW observatories owing to the short initial orbital periods (see Fig. 7), and they would be also observable as binary radio pulsars before the mass-transfer process.[6] Meanwhile, the preceding detached NS+He star systems could be detectable optically as He stars are relatively luminous objects. By considering the contribution of the WD/MS donor channels (e.g. Tauris 2018; Paper I), the He star donor channel approximately accounts for one-third of UCXBs theoretically on the basis of this work. This indicates that we cannot ignore the contribution of the He star donor channel in forming UCXBs. We note that accretion-induced collapse of ONe WDs can also produce NS systems, likely contributing to the formation of UCXBs (for a recent review see Wang & Liu 2020; see also Tauris et al. 2013; Ablimit & Li 2015; Wang 2018; Ablimit 2019).

Aside from the contribution to the formation of UCXBs, NS+He star systems also produce intermediate-mass binary pulsars (IMBPs). Chen & Liu (2013) studied NS+He star systems to form IMBPs with short orbital periods (<3 d), in which a He star transfers its material on to the surface of a NS when it evolves to the subgiant stage, resulting in a recycling process for the NS. Tang, Liu & Wang (2019) recently found that NS+He star systems can reproduce the observed parameters of PSR J0621+1002 that is one of the well-observed IMBPs. It is worth noting that NS+He star systems close to the right-hand boundary in Fig. 8 can also form UCXBs when the He stars evolve to the subgiant stage, turning into IMBPs (detached NS+CO WD binaries) at the end. The detached NS+CO WD binaries then may spiral in, experience unstable mass transfer, and merge, producing transient supernova-like events (e.g. Bobrick, Davies & Church 2017). If the mass transfer is stable from CO WDs to NSs, the binaries will experience UCXB phase again.

In addition, Shao, Li & Dai (2019) suggested that NS+He star systems can significantly contribute to the population of ultraluminous X-ray sources if the NS accretes He-rich material with a super-$\dot{M}_{\rm Edd}$ (see also Abdusalam et al. 2020). Furthermore, Ma et al. (2020) recently studied Type I X-ray bursts from NSs that accrete He-rich matter, resulting in intermediate X-ray bursts in observations. Compared with normal X-ray bursts, Ma et al. (2020) found that the intermediate X-ray bursts have longer recurrence time-scales and higher luminosities.

6 SUMMARY

The origin of UCXBs is still highly uncertain. In this work, by combining detailed stellar evolution calculations and BPS approach, we simulated the formation and evolution of UCXBs through the He star donor channel in a systematic way. We first explored the parameter spaces for producing UCXBs in the orbital period–secondary mass plane using detailed binary evolution calculations, and then used these results to carry out a series of Monte Carlo BPS simulations. The main conclusions are summarized as follows.

(i) We found that all NS+He star systems for producing UCXBs can be visible as the *LISA* sources within a distance of 15 kpc. We estimate the rates of UCXB-*LISA* sources in the Galaxy $\sim$3.1–11.9 Myr^{-1}. Calibrating by the UCXB observations, we expect that the number of UCXB-*LISA* sources can reach about 1–26 in the Galaxy.

(ii) The evolutionary tracks of UCXBs through the He star donor channel are able to explain the location of the five transient sources with relatively long orbital periods quite well, especially for Swift J1756.9−2508.

(iii) We found that the relation in the diagram between the mass-transfer rate on the descending stage and the orbital period can be used to distinguish different channels for the formation of UCXBs.

(iv) The preceding detached NS+He star systems forming UCXBs can be detected by the future GW observatories like *LISA*, *Taiji*, and *TianQin*. They would be also observable as binary radio pulsars.

(v) When the He stars fill their Roche lobes, the NS+He star binaries appear to be UCXBs and GW sources simultaneously. The NS+He star systems appear to be UCXBs with lifetime about 1.5–4.0 Gyr, in which they show as persistent sources lasting for about 40–80 Myr.

(vi) After the UCXB stage, the evolved NS systems studied in this work will show as millisecond radio pulsars, eventually forming single millisecond radio pulsars or pulsar+planet-like systems.

ACKNOWLEDGEMENTS

We acknowledge the anonymous referee for valuable comments that help to improve the paper. This study is partly supported by the NSFC (Nos 11521303, 12090040/3, 11573016, 11733009, 11873085, 12073071, 11903075, and 12003013), the science research grants from the China Manned Space Project (Nos CMS-CSST-2021-A13/B07), the Program for Innovative Research Team (in Science and Technology) at the University of Henan Province, the Youth Innovation Promotion Association CAS (Nos 2018076 and 2021058), the Western Light Youth Project of CAS, and the Yunnan Fundamental Research Projects (Nos 202001AT070058, 2019FJ001, and 202001AS070029).

DATA AVAILABILITY

The data of the numerical calculations in this paper can be made available on request by contacting BW.

REFERENCES

Abbott B. P. et al., 2016, Phys. Rev. Lett., 116, 061102
Abbott B. P. et al., 2017, Phys. Rev. Lett., 119, 141101
Abdusalam K., Ablimit I., Hashim P., Lü G.-L., Mardini M. K., Wang Z.-J., 2020, ApJ, 902, 125
Ablimit I., 2019, ApJ, 881, 72
Ablimit I., Li X.-D., 2015, ApJ, 800, 98
Alpar M. A., Cheng A. F., Ruderman M. A., Shaham J., 1982, Nature, 300, 728
Amaro-Seoane P. et al., 2017, preprint (arXiv:1702.00786)
Bahramian A. et al., 2017, MNRAS, 467, 2199
Bailes M. et al., 2011, Science, 333, 1717

[6]Actually, NSs with an ellipticity can also possibly appear as high-frequency GW sources, i.e. the detached NS+He star systems have an opportunity to become dual-line GW sources (see Tauris 2018; Chen 2021; Suvorov 2021).

Bailyn C. D., Grindlay J. E., 1987, ApJ, 316, L25
Bao J. et al., 2019, Phys. Rev. D, 100, 084024
Bauer E. B., Kupfer T., 2021, ApJ, submitted, preprint (arXiv:2106.13297)
Belczynski K., Taam R. E., 2004, ApJ, 603, 690
Bisnovatyi-Kogan G. S., 1989, Astrophysics, 31, 751
Bobrick A., Davies M. B., Church R. P., 2017, MNRAS, 467, 3556
Cartwright T. F. et al., 2013, ApJ, 768, 183
Chen H.-L., Chen X., Tauris T. M., Han Z., 2013, ApJ, 775, 27
Chen H.-L., Tauris T. M., Han Z., Chen X., 2021, MNRAS, 503, 3540
Chen W.-C., 2020, ApJ, 896, 129
Chen W.-C., 2021, Phys. Rev. D, 103, 103004
Chen W.-C., Li X.-D., Xu R.-X., 2011, A&A, 530, A104
Chen W.-C., Liu D., Wang B., 2020, ApJ, 900, L8(Paper I)
Chen W.-C., Liu W.-M., 2013, MNRAS, 432, L75
Chen W.-C., Podsiadlowski P., 2016, ApJ, 830, 131
Chen X., Han Z., 2003, MNRAS, 341, 662
Chen X., Maxted P. F. L., Li J., Han Z., 2017, MNRAS, 467, 1874
Coti Zelati F. et al., 2021, A&A, 650, A69
Cumming A., 2003, ApJ, 595, 1077
Davies M. B., Benz W., Hills J. G., 1992, ApJ, 401, 246
Davies M. B., Hansen B. M. S., 1998, MNRAS, 301, 15
Deloye C. J., Bildsten L., 2003, ApJ, 598, 1217
Deng Z.-L., Li X.-D., Gao Z.-F., Shao Y., 2021, ApJ, 909, 174
Dewi J. D. M., Pols O. R., Savonije G. J., van den Heuvel E. P. J., 2002, MNRAS, 331, 1027
Dubus G., Lasota J., Hamcury J., Charles P., 1999, MNRAS, 303, 139
Ergma E., 1996, A&A, 315, L17
Galloway D. K., Muno M. P., Hartman J. M., Psaltis D., Chakrabarty D., 2008, ApJS, 179, 360
Ge H., Webbink R. F., Chen X., Han Z., 2020, ApJ, 899, 132
Han Z., 2008, ApJ, 677, L109
Han Z., Ge H., Chen X., Chen H., 2020, Res. Astron. Astrophys., 20, 161
Han Z., Podsiadlowski Ph., Eggleton P. P., 1995, MNRAS, 272, 800
Han Z., Podsiadlowski Ph., Maxted P. F. L., Marsh T. R., Ivanova N., 2002, MNRAS, 336, 449
Han Z., Tout C. A., Eggleton P. P., 2000, MNRAS, 319, 215
Heinke C. O. et al., 2013, ApJ, 768, 184
Hjellming M. S., Webbink R. F., 1987, ApJ, 318, 794
Huang S.-J. et al., 2020, Phys. Rev. D, 102, 063021
Hurley J. R., Tout C. A., Pols O. R., 2002, MNRAS, 329, 897
Iben I. J., Tutukov A. V., Yungelson L. R., 1995, ApJS, 100, 233
in't Zand J. J. M., Jonker P. G., Markwardt C. B., 2007, A&A, 465, 953
Istrate A. G., Tauris T. M., Langer N., 2014, A&A, 571, A45
Ivanova N. et al., 2010, ApJ, 717, 948
Ivanova N. et al., 2013, A&AR, 21, 59
Ivanova N., Rasio F. A., Lombardi J. C., Dooley K. L., Proulx Z. F., 2005, ApJ, 621, L109
Jia K., Li X.-D., 2015, ApJ, 814, 74
Jiang L., Chen W.-C., Li X.-D., 2017, ApJ, 837, 64
King A. R., Kolb U., Burderi L., 1996, ApJ, 464, L127
Koliopanos F., Péault M., Vasilopoulos G., Webb N., 2021, MNRAS, 501, 548
Kremer K., Breivik K., Larson S. L., Kalogera V., 2017, ApJ, 846, 95
Kruckow M. U., Neunteufel P. G., Di Stefano R., Gao Y., Kobayashi C., 2021, ApJ, in press (arXiv:2107.05221)
Landau L. D., Lifshitz E. M., 1971, Classical Theory of Fields. Pergamon Press, Oxford
Lasota J.-P., Dubus G., Kruk K., 2008, A&A, 486, 523
Li X.-D., 2002, ApJ, 564, 930
Li X.-D., 2015, New Astron. Rev., 64, 1
Licquia T., Newman J., 2014, Am. Astron. Soc. Meeting Abstr., 223, 336.04
Lin J., Rappaport S., Podsiadlowski P., Nelson L., Paxton B., Todorov P., 2011, ApJ, 732, 70
Lin J., Yu W., 2018, MNRAS, 474, 1922
Liu Q. Z., van Paradijs J., van den Heuvel E. P. J., 2007, A&A, 469, 807
Liu W.-M., Jiang L., Chen W.-C., 2021, ApJ, 910, 22
Lü G., Zhu C., Wang Z., Iminniyaz H., 2017, ApJ, 847, 62
Luo J. et al., 2016, Classical Quantum Gravity, 33, 035010
Luo Z. et al., 2020, Results Phys., 16, 102918
Ma B., Li X.-D., 2009a, ApJ, 691, 1611
Ma B., Li X.-D., 2009b, ApJ, 698, 1907
Ma Y.-C., Liu H.-L., Zhu C.-H., Wang Z.-J., Li L., Lü G.-L., 2020, Res. Astron. Astrophys., 20, 049
Martin R. G., Livio M., Palaniswamy D., 2016, ApJ, 832, 122
Miller G. E., Scalo J. M., 1979, ApJS, 41, 513
Nelemans G., 2005, in Hameury J.-M., Lasota J.-P., eds, ASP Conf. Ser. Vol. 330, The Astrophysics of Cataclysmic Variables and Related Objects. Astron. Soc. Pac., San Francisco, p. 27
Nelemans G., 2009, Classical Quantum Gravity, 26, 094030
Nelemans G., Jonker P. G., 2010, New Astron. Rev., 54, 87
Nelemans G., Jonker P. G., Marsh T. R., van der Klis M., 2004, MNRAS, 348, L7
Nelemans G., Jonker P. G., Steeghs D., 2006, MNRAS, 370, 255
Nelemans G., Yungelson L. R., van der Sluys M. V., Tout C. A., 2010, MNRAS, 401, 1347
Nelson L. A., Rappaport S. A., Joss P. C., 1986, ApJ, 304, 231
Paczyński B., 1976, in Eggleton P. P., Mitton S. M., Whelan J. A. J., eds, Proc. IAU Symp. 73, Structure and Evolution of Close Binaries Systems. Reidel, Dordrecht, p. 75
Paxton B. et al., 2013, ApJS, 208, 4
Paxton B. et al., 2015, ApJS, 220, 15
Paxton B. et al., 2018, ApJS, 234, 34
Paxton B. et al., 2019, ApJS, 243, 10
Paxton B., Bildsten L., Dotter A., Herwig F., Lessafre P., Timmes F., 2011, ApJS, 192, 3
Peng S., Shen R.-F., 2021, ApJ, in press (arXiv:2105.13613)
Pietrukowicz P., Mróz P., Udalski A., Soszyński I., Skowron J., 2019, ApJ, 881, L41
Podsiadlowski P., 1993, in Phillips J. A., Thorsett S. E., Kulkarni S. R., eds, ASP Conf. Ser. Vol. 36, Planets Around Pulsars. Astron. Soc. Pac., San Francisco, p. 149
Podsiadlowski P., Han Z., Rappaport S., 2003, MNRAS, 340, 1214
Podsiadlowski P., Rappaport S., Pfahl E. D., 2002, ApJ, 565, 1107
Pringle J. E., Webbink R. F., 1975, MNRAS, 172, 493
Pylyser E. H. P., Savonije G. J., 1988, A&A, 191, 57
Pylyser E. H. P., Savonije G. J., 1989, A&A, 208, 52
Rappaport S., Joss P.∼C., Webbink R.∼F., 1982, ApJ, 254, 616
Robson T., Cornish N. J., Liu C., 2019, Classical Quantum Gravity, 36, 105011
Ruan W.-H., Liu C., Guo Z.-K., Wu Y.-L., Cai R.-G., 2020, Nat. Astron., 4, 108
Ruan W.-H., Liu C., Guo Z.-K., Wu Y.-L., Cai R.-G., 2021, Research, 2021, 6014164
Ruderman M. A., Shaham J., 1985, ApJ, 289, 244
Ruderman M., Shaham J., Tavani M., 1989, ApJ, 336, 507
Savonije G. J., de Kool M., van den Heuvel E. P. J., 1986, A&A, 155, 51
Sazonov S. et al., 2020, New Astron. Rev., 88, 101536
Sengar R., Tauris T. M., Langer N., Istrate A. G., 2017, MNRAS, 470, L6
Shao Y., Li X.-D., 2012, ApJ, 756, 85
Shao Y., Li X.-D., 2015, ApJ, 809, 99
Shao Y., Li X.-D., Dai Z.-G., 2019, ApJ, 886, 118
Soker N., 2013, New Astron., 18, 18
Soker N., Grichener A., Sabach E., 2018, ApJ, 863, L14
Solheim J. E., 2010, PASP, 122, 1133
Suvorov A. G., 2021, MNRAS, 503, 5495
Tang W., Li X.-D., 2021, MNRAS, 506, 3323
Tang W., Liu D., Wang B., 2019, MNRAS, 490, 752
Tauris T. M., 2018, Phys. Rev. Lett., 121, 131105
Tauris T. M., Sanyal D., Yoon S.-C., Langer N., 2013, A&A, 558, A39
Tauris T. M., van den Heuvel E. P. J., 2006, in Lewin W. H. G., van der Klis M., eds, Compact Stellar X-ray Sources. Cambridge Univ. Press, Cambridge, p. 623
Tudor V. et al., 2018, MNRAS, 476, 1889
Tutukov A. V., Yungelson L. R., 1993, Astron. Rep., 37, 411
van den Heuvel E. P. J., van Paradijs J., 1988, Nature, 334, 227
van der Sluys M. V., Verbunt F., Pols O. R., 2005a, A&A, 431, 647

van der Sluys M. V., Verbunt F., Pols O. R., 2005b, A&A, 440, 973
van Haaften L. M., Nelemans G., Voss R., Wood M. A., Kuijpers J., 2012a, A&A, 537, A104
van Haaften L. M., Nelemans G., Voss R., Jonker P. G., 2012b, A&A, 541, A22
van Haaften L. M., Voss R., Nelemans G., 2012c, A&A, 543, A121
Van K. X., Ivanova N., Heinke C. O., 2019, MNRAS, 483, 5595
Verbunt F., 1987, ApJ, 312, L23
Verbunt F., 2005, in Burderi L., Antonelli L. A., D'Antona F., Di Salvo T., Israel G. L., Piersanti L., Tornambè A., Straniero O., eds, AIP Conf. Proc., Vol. 797, Interacting Binaries: Accretion, Evolution, and Outcomes. Am. Inst. Phys., New York, p. 30
Wang B., 2018, MNRAS, 481, 439
Wang B., Chen X., Meng X., Han Z., 2009, ApJ, 701, 1540
Wang B., Liu D., 2020, Res. Astron. Astrophys., 20, 135
Wang B., Podsiadlowski P., Han Z., 2017, MNRAS, 472, 1593
Wang H.-T. et al., 2019, Phys. Rev. D, 100, 043003
Warner B., 1995, Ap&SS, 225, 249
Webbink R. F., 1984, ApJ, 277, 355
Werner K., Nagel T., Rauch T., Hammer N. J., Dreizler S., 2006, A&A, 450, 725
Willems B., Kolb U., 2004, A&A, 419, 1057
Wong T. L. S., Schwab J., 2019, ApJ, 878, 100
Xu X.-J., Li X.-D., 2007, A&A, 476, 1283
Yu S., Lu Y., Jeffery C. S., 2021, MNRAS, 503, 2776
Yungelson L. R., 2008, Astron. Lett., 34, 620
Yungelson L. R., Nelemans G., van den Heuvel E. P. J., 2002, A&A, 388, 546
Zhong J., Wang Z., 2011, ApJ, 729, 8
Zhu C.-H., Lü G.-L., Wang Z.-J., 2012, Res. Astron. Astrophys., 12, 1526

This paper has been typeset from a TEX/LATEX file prepared by the author.